

UDC 621.521

Oleksandr Levchenko*

National University «Yuri Kondratyuk Poltava Polytechnic»

<https://orcid.org/0009-0004-3191-7097>

Oleksandr Ivakhno

National University «Yuri Kondratyuk Poltava Polytechnic»

<https://orcid.org/0009-0005-9375-8041>

Theoretical substantiation of the parameters of the concrete batching plant feeding system for stabilising the mass flow rate of moist materials

Abstract. The article presents a theoretical substantiation of the parameters of the feeding system of a concrete batching plant for stabilising the mass flow rate of moist fine aggregate with a particle size of 0–5 mm. It has been established that, at a sand moisture content of $W \geq 4\text{--}6\%$, the standard hopper geometry with a wall inclination angle of $\alpha = 60^\circ$ does not ensure mass flow according to the Jenike criterion, resulting in the formation of dynamic arches and a pulsating material discharge with a coefficient of variation of $CV = 15\text{--}25\%$. A scientific hypothesis is proposed that the flow regime can be converted from funnel flow to mass flow by artificially reducing the effective internal friction angle below its critical value through the mechanical disruption of capillary bonds using an active loosening device with a horizontal shaft and pins arranged at 90° angular intervals. Based on the theory of limit equilibrium and the Janssen equation incorporating cohesion, an analytical model describing the formation of dynamic arches was developed, and a design equation for the critical angular velocity (ω_{cr}) was derived. An integrated mathematical model of the material mass flow rate was also established. It was found that, at an operating angular velocity of $\omega_{op} \geq 2.5\omega_{cr}$, the coefficient of variation of the mass flow rate reaches $CV_0 \leq 3\%$ for $W \leq 6\%$, satisfying the requirements of DSTU B V.2.7-96:2000.

Keywords: concrete batching plant, loosening device, arching, cohesion, moisture content, batching, hopper, mass flow rate, angular velocity, material flow

*Corresponding author E-mail: pbuidceh@gmail.com



Copyright © The Author(s). This is an open access article distributed under the terms of the Creative Commons Attribution-NonCommercial-ShareAlike 4.0 International License. (<https://creativecommons.org/licenses/by-nc-sa/4.0/>)

Received: 08.02.2026

Accepted: 12.04.2026

Published: 31.05.2026

Introduction.

The consistency of aggregate dosing is a key factor in the quality of concrete mixes at concrete mixing plants (CMPs). According to the requirements of DSTU B V.2.7-96-2000 [1], the deviation in the mass flow rate of bulk components must not exceed 3%. However, under production conditions with high sand moisture content, this standard is systematically violated.

Operational experience with CMPs shows that when sand moisture content $W \geq 4 - 6\%$, dynamic arching occurs in the feed system hoppers, blocking the flow of material. The result is a pulsating feed with a coefficient of variation $CV = 15 - 25\%$ and emergency shutdowns of the process [2, 3]. The root cause of this phenomenon is a physical change in the rheological properties of moist bulk material: an increase in the effective angle of internal friction ϕ_w and cohesion

$C(W)$ due to the formation of liquid menisci between grains [4, 5].

Existing approaches to solving the problem - increasing the angle of the hopper walls or installing vibrators - have significant design and energy limitations [6, 7]. A promising direction is the use of active mechanical loosening devices that directly break the capillary bonds between material particles above the discharge opening [8].

Problem statement

The purpose of this article is to provide a theoretical justification for the parameters of the active loosener in the CMPs feeding system to ensure a stable mass flow rate of moist, fine-grained aggregates in the 0 - 5 mm fraction in accordance with regulatory requirements of $CV_0 \leq 3\%$.

To achieve this goal, it is necessary to: establish the physical-mechanical mechanism of dynamic arch

formation in bunkers containing moist materials; develop an analytical model of the influence of the kinematic parameters of a horizontal-shafted loosener on the material flow regime; and derive analytical relationships for determining the threshold angular velocity ω_{cr} and the mass flow rate of the material.

Main material and results.

Analysis results demonstrate that the root cause of batching plant (BP) productivity instability is the physical change of flow regime of moist bulk materials in hoppers. At sand moisture $W > 5-6\%$, the standard geometry of production hoppers (wall inclination angle $\alpha = 55-65^\circ$) does not satisfy the conditions for mass flow regime according to the Jenike criterion [9, 10], leading to the formation of dynamic arches and pulsating material feed.

The condition for mass flow regime is that the hopper geometry and physical properties of the material satisfy the inequality [10]:

$$\varphi_w \leq \varphi_{cr} = f(\delta, \alpha, \mu_w) \quad (1)$$

where φ_w – effective internal friction angle of the material at moisture W , deg;

φ_{cr} – critical friction angle for mass flow regime, deg;

α – wall inclination angle of the hopper, deg;

μ_w – wall friction coefficient of the material.

The relationship between moisture W and effective internal friction angle φ_w for construction sand [4]:

$$\varphi_w = \varphi_0 + kW \cdot W^n \quad (2)$$

where $\varphi_0 = 17-19^\circ$ – friction angle of dry material;

$kW \approx 1.8-2.2$ – empirical coefficient; $n \approx 0.7-0.9$;

W – absolute moisture content, %.

Table 1 – Dependence of effective internal friction angle of sand on moisture content and flow regime ($\alpha = 60^\circ$, construction sand $d = 0.5-2.0$ mm)

Moisture W , %	Bulk density ρ , kg/m^3	Effective friction angle φ_w , deg	Wall friction coefficient μ_w	Flow regime
0 (dry)	1550–1600	17–19	0.30–0.35	Mass flow
2	1480–1520	21–25	0.38–0.45	Mass/ transitional
4	1400–1450	28–33	0.47–0.55	Funnel flow
6	1410–1460	33–38	0.55–0.63	Funnel flow
8	1600–1650	37–42	0.60–0.68	Funnel flow
10–12	1720–1800	40–46	0.62–0.70	Funnel flow

Data in Table 1 confirm: at $W \geq 4\%$, the sand friction angle reaches $28-33^\circ$, which for a hopper with $\alpha = 60^\circ$ corresponds to funnel flow regime. Returning to mass flow by changing the wall angle would require $\alpha \geq 75-85^\circ$, which is structurally impractical [9, 10].

Based on the foregoing, a scientific hypothesis is formulated: transitioning the flow regime of moist bulk materials from funnel flow to mass flow without changing the standard geometry of BP hoppers ($\alpha = 60^\circ$) is possible by artificially reducing the effective internal friction angle φ_w below the critical value φ_{cr} – through continuous mechanical destruction of capillary bonds between particles directly above the discharge outlet by an active loosener, whose pins are positioned with 90° angular offset and rotate at a frequency exceeding the threshold value ω_{cr} .

The mechanical action of the loosener is described by the concept of reduced effective angle φ_{eff} :

$$\varphi_{eff} = \varphi_w - \Delta\varphi(\omega, R_p) \quad (3)$$

where $\Delta\varphi(\omega, R_p)$ – decrement of reduction of the effective friction angle under the action of the loosener as a function of angular velocity ω (rad/s) and pin length R_p (m). The condition for transition to mass flow:

$$\Delta\varphi(\omega, R_p) > \varphi_w - \varphi_{cr} = \Delta\varphi_{required} \quad (4)$$

The appearance of surface moisture leads to the formation of liquid menisci in contact zones between particles. The capillary adhesion force between two

spherical particles of radius r forming a toroidal meniscus is determined by the relation [4, 11]:

$$F_{cap} = 2\pi \cdot r \cdot \sigma \cdot \cos \theta + \pi \cdot r^2 \cdot \Delta P_c \quad (5)$$

where r – mean radius of sand grain, m;

$\sigma = 0.0728$ N/m – water surface tension coefficient at $T = 20^\circ\text{C}$;

$\theta \approx 0^\circ$ – contact angle of wetting of quartz sand;

ΔP_c – pressure difference in the meniscus, Pa, determined by the Laplace equation [11]:

$$\Delta P_c = \sigma \cdot \left(\frac{1}{R_1} + \frac{1}{R_2} \right) \quad (6)$$

where R_1, R_2 – principal radii of curvature of the meniscus, m. For typical construction sand grains ($d = 0.5-2.0$ mm) at $W = 4-6\%$, the specific capillary force is $100-500$ Pa.

The relationship between moisture W and cohesion $C(W)$ of the material layer:

$$C(W) = C_0 + \beta \cdot W^m \quad (7)$$

where $C_0 \approx 0$ Pa – residual cohesion of absolutely dry material;

$\beta \approx 120-180$ Pa/% – capillary hardening coefficient;

$m \approx 0.8-1.2$ – exponent.

The increase of cohesion with increasing W is the primary cause of arch formation, as confirmed by calculated dependencies for various sand fractions (Fig. 1).

Vertical stress at depth z from the material surface in the hopper is described by the Janssen equation accounting for cohesion [10]:

$$\sigma v(z) = \frac{\rho \cdot g \cdot Rh}{kw \cdot \mu} \cdot \left[1 - \exp\left(-kw \cdot \mu \cdot \frac{z}{Rh}\right) \right] + \frac{C(W)}{\mu \cdot kw} \quad (8)$$

where ρ – bulk density of material, kg/m³;
 g – gravitational acceleration, m/s²;

$Rh = B \cdot L / [2 \cdot (B + L)]$ – hydraulic radius of the hopper cross-section, m;

$kw = (1 - \sin \varphi_w) / (1 + \sin \varphi_w)$ – lateral pressure coefficient (Rankine coefficient);

μ – wall friction coefficient.

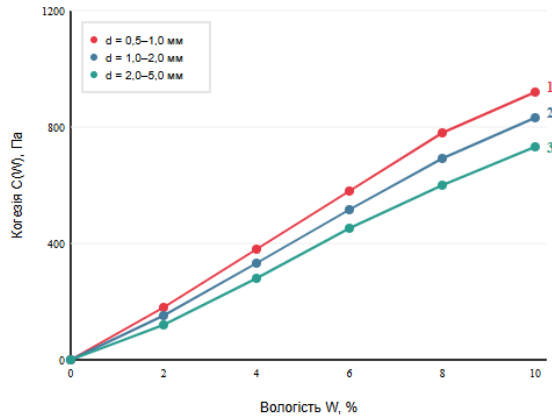


Figure 1 – Calculated dependence of sand cohesion $C(W)$ on absolute moisture content for various fractions (formula 2.7): 1 – $d = 0.5\text{--}1.0$ mm; 2 – $d = 1.0\text{--}2.0$ mm; 3 – $d = 2.0\text{--}5.0$ mm. The increase of cohesion with increasing W is the primary cause of arch formation.

A dynamic arch forms when horizontal compressive stresses σh in the thin layer of material directly above the discharge outlet exceed the shear failure stress τf . Equilibrium condition for an arch in the form of a parabolic arch over an outlet of width B [9]:

$$\sigma h \geq \tau f = C(W) + \sigma n \cdot \tan(\varphi_w) \quad (9)$$

where σn – normal stress in the arch plane, Pa;

φ_w – effective internal friction angle at moisture W , deg. Substituting (2.8) into (2.9) and transforming gives the critical outlet width B_{cr} , below which the arch is stable [9]:

$$B_{cr} = 2 \cdot C(W) \cdot \frac{(1 + \sin \varphi_w)}{[\rho \cdot g \cdot \sin \varphi_w \cdot (1 - \sin \varphi_w)]} \quad (10)$$

At $B > B_{cr}$ – the arch is unstable and collapses on its own; at $B < B_{cr}$ – the arch is stable.

Data in Table 2 show: at $W \geq 6\%$, the value $B_{cr} = 510\text{--}680$ mm exceeds the smaller side of the standard BP hopper outlet (300 mm), which guarantees the formation of stable arches without external mechanical intervention (Fig. 2). This directly confirms the impossibility of ensuring stable discharge of moist fine-grained material from a standard BP hopper without additional technical means.

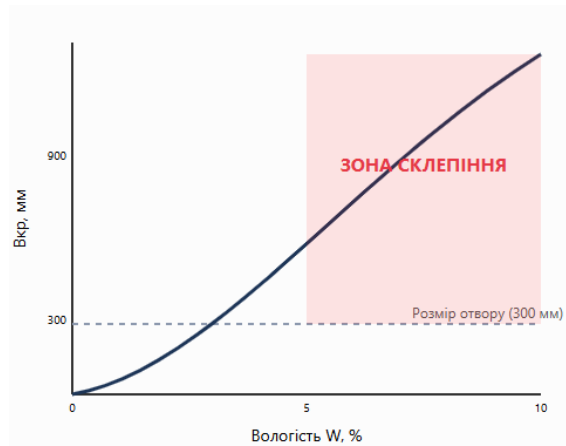


Figure 2 – Dependence of critical discharge outlet width B_{cr} on material moisture content for various fractions (formula 9). Dashed line – actual smaller dimension of BP hopper outlet (300 mm); at $W \geq 5\text{--}6\%$, B_{cr} exceeds 300 mm for all three fractions.

The design feature of the loosener consists in the arrangement of pins on the central shaft with 90° angular offset between adjacent pairs and horizontal shaft orientation. With a horizontal shaft, the plane of pin rotation coincides with the vertical plane YZ , the gravity vector g lies in this plane, ensuring uniform load on the shaft per revolution.

Table 2 – Critical discharge outlet width B_{cr} for construction sand ($\rho = 1450$ kg/m³, $g = 9.81$ m/s², formula 2.10)

W, %	C(W), Pa	φ_w , deg	B_{cr} , mm	Status of 800×300 mm outlet
0	≈ 0	17–19	≈ 0	Free flow
2	120–180	21–25	180–260	Free flow
4	280–380	28–33	380–490	Arch possible
6	450–580	33–38	510–680	Stable arch
8	600–780	37–42	640–870	Stable arch
10	750–920	40–46	780–1050	Stable arch

For four adjacent pins ($i = 1, 2, 3, 4$), polar angles in the plane of rotation:

$$\theta_i(t) = \omega \cdot t + (i - 1) \cdot \frac{\pi}{2}, \quad i = 1, 2, 3, 4 \quad (11)$$

This configuration guarantees that any point on a circle of radius R_p in the rotation plane is crossed by the trajectory of at least one pin every $\Delta t = \pi / (2\omega)$ seconds. The condition for complete coverage of the arch formation zone is:

$$R_p \geq \frac{B_{cr}}{2} \quad (12)$$

For a hopper 800×300 mm at $W_{max} = 8\%$: $R_p \geq 150$ mm. Uniform arrangement of pins with 90° angular offset provides a load uniformity coefficient $k_{uniform} \approx 0.85\text{--}0.87$ compared to $k_{uniform} \approx 0.60$ for the non-uniform scheme (2 pins at 180°), which reduces peak drive load by 28% (Fig. 3).

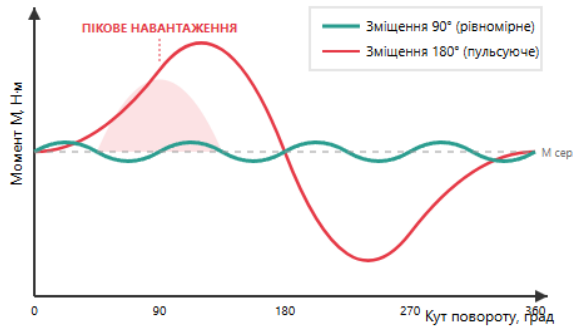


Figure. 3 – Comparison of torque on the loosener shaft: uniform 90° placement (green curve) provides minimal load oscillations (CV ≈ 15%) compared to the non-uniform scheme (red curve, CV ≈ 60%). Shaded area – peak shaft overload for the non-uniform scheme.

Resistance force of material to relative movement of a cylindrical pin [14]:

$$F_{res} = k_{res} \cdot C(W) \cdot dp \cdot L_p \cdot vp^2 \quad (13)$$

where $k_{res} \approx 1.0-1.3$ – dimensionless resistance coefficient;

$C(W)$ – material cohesion, Pa;

dp – pin diameter;

$L_p = R_p - r_v$ – pin length;

$vp = \omega \cdot r_p$ – linear velocity of pin tip. Shear stress developed by the pin in the material at radius r :

$$\begin{aligned} \tau_{loosen}(r) &= \frac{F_{res}}{dp \cdot L_p} = \\ &= k_{res} \cdot C(W) \cdot (\omega \cdot r)^2 \end{aligned} \quad (14)$$

The arch destruction condition, with substitution of (14) and introduction of correction coefficient $k_c = 1 + \sigma_n/C(W) \approx 2.0-3.5$, gives the design formula for threshold angular velocity ω_{cr} :

$$\omega_{cr} \geq \sqrt{\left[\tan(\varphi_w - \varphi_{cr}) \cdot \frac{g \cdot k_c}{(k_{res} \cdot R_p^2)} \right]} \quad (15)$$

where in the simplified calculation $k_c = 1$ (conservative estimate).

Expression (15) relates the kinematic parameters of the loosener (ω_{cr} , R_p) to the physical properties of the material (φ_w , determined by moisture W via formula 2).

Table 3 – Threshold angular velocity ω_{cr} and rotation speed n_{cr} for construction sand ($k_{res} = 1.1$, $k_c = 1$, $\varphi_{cr} = 25^\circ$, horizontal shaft)

W, %	$R_{ш}$, m	φ_w , deg	$\varphi_w - \varphi_{cr}$, deg	ω_{cr} , rad/s	n_{cr} , rpm
4	0.10	30	5	9.4	90
4	0.15	30	5	6.3	60
6	0.10	35	10	13.6	130
6	0.15	35	10	9.1	87
6	0.20	35	10	6.8	65
8	0.15	39	14	10.8	103
8	0.20	39	14	8.1	77
10	0.15	43	18	12.2	117
10	0.20	43	18	9.1	87

Data in Table 3 are a primary engineering tool for selecting loosener parameters. Key design recommendation: doubling R_p (from 0.10 to 0.20 m) halves ω_{cr} at constant moisture (Fig. 4).

Interpretation of results and their approval.

The classical base is the Beverloo formula [12]:

$$Q^0 = Cd \cdot \rho \cdot \sqrt{g} \cdot (B - k \cdot dp)^{\frac{5}{2}} \quad (16)$$

where Q_0 – mass flow rate in mass flow regime, kg/s; $Cd \approx 0.60-0.70$ – empirical discharge coefficient for slot outlet;

B – outlet width, m;

$k \approx 1.5$ – grain size coefficient;

dp – mean particle diameter, m.

At elevated moisture, the discharge coefficient Cd decreases due to capillary cohesion. Based on experimental data and results from [13], the following modified dependence is proposed:

$$\begin{aligned} Cd(W) &= Cd^0 \cdot \exp(-\lambda \cdot W), \\ \lambda &\approx 0.07 - 0.12 \%^{-1} \end{aligned} \quad (17)$$

where the parameter λ for construction sand $d = 0.5-2.0$ mm: $\lambda \approx 0.091 \%^{-1}$. At $W > W_{cr} \approx 5.5\%$, flow is completely blocked by an arch: $Q \rightarrow 0$.

When the loosener operates at $\omega \geq \omega_{cr}$, the loosener efficiency coefficient $\eta(\omega)$ is introduced:

$$\begin{aligned} \eta(\omega) &= 1 - \exp\left(-k\eta \cdot \frac{\omega - \omega_{cr}}{\omega_{cr}}\right), \\ &\text{at } \omega \geq \omega_{cr} \end{aligned} \quad (18)$$

where $k\eta \approx 2.0-3.5$ – loosener efficiency coefficient. At $\omega < \omega_{cr}$: $\eta(\omega) = 0$ – the loosener does not ensure mass flow. Mass flow rate with loosener operation:

$$\begin{aligned} Q_r(W, \omega) &= Q^0 \cdot \left[\exp(-\lambda \cdot W) \times \right. \\ &\quad \left. \times (1 - \eta(\omega)) + \eta(\omega) \right] \end{aligned} \quad (19)$$

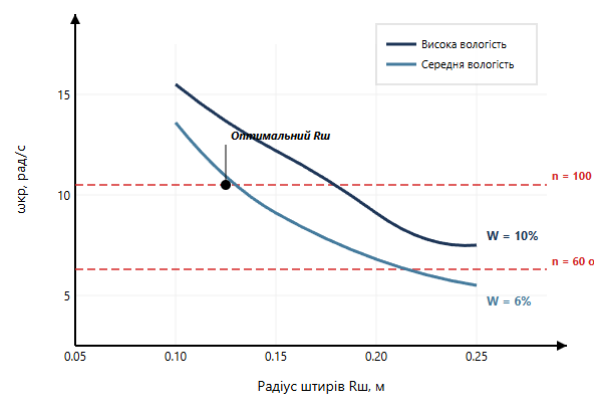


Figure. 4 – Dependence of critical angular velocity ω_{cr} on pin radius R_p at various sand moisture levels (formula 2.20, $k_{res} = 1.1$, $k_c = 1$). Horizontal dashed lines – practically achievable values for standard gearmotor series.

At $\omega \gg \omega_{cr}$: $\eta(\omega) \rightarrow 1$, and $Q_r \rightarrow Q_0 = \text{const}$ – mass flow rate becomes independent of material moisture W . This is the mathematical formulation of the proposed scientific hypothesis (Fig. 5).

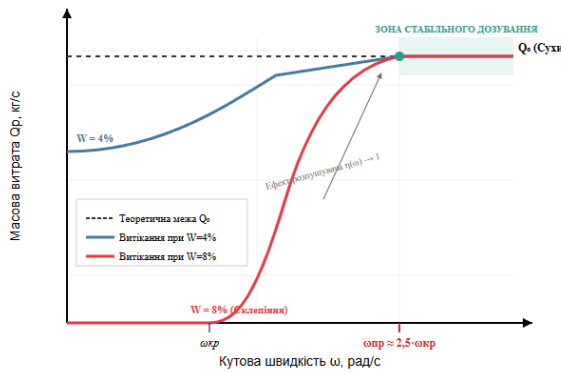


Figure 5. Theoretical dependences of mass flow rate Q_r on loosener angular velocity ω at various sand moisture levels (model 2.25, $R_p = 0.15$ m, $B = 0.30$ m, horizontal shaft). At $\omega > 2.5 \cdot \omega_{cr}$, curves for all moisture levels merge into a single horizontal line $Q_0 = \text{const}$.

$$Q_r(W, \omega, R_p) = C d^0 \cdot \rho \cdot \sqrt{g} \cdot (B - k \cdot dp)^{\frac{5}{2}} \times \left\{ \exp(-\lambda \cdot W) \cdot \exp \left[-k\eta \cdot \left(\frac{\omega}{\omega_{cr}(W)} - 1 \right) \right] + 1 - \exp \left[-k\eta \cdot \left(\frac{\omega}{\omega_{cr}(W)} - 1 \right) \right] \right\} \quad (21)$$

where $\omega_{cr}(W)$ is calculated by formula (20) for the given moisture W .

Table 4 – Theoretical mass flow rate Q_r and coefficient of variation CV_Q depending on loosener operating mode ($B = 0.30$ m, $\rho = 1500$ kg/m³, $dp = 1.0$ mm, $k\eta = 2.8$, $R_p = 0.15$ m)

W, %	Q without loosener, kg/s	Q at ω_{cr} , kg/s	Q at $1.5\omega_{cr}$	Q at $2.5\omega_{cr}$	CV_Q at $2.5\omega_{cr}$, %
0	8.35	8.35	8.35	8.35	0.0
2	7.23	7.55	8.10	8.28	0.8
4	5.41	6.80	7.94	8.22	1.6
6	3.87	5.72	7.65	8.15	2.4
8	2.75	4.68	7.38	8.07	3.4 *
10	1.96	3.65	7.12	7.98	4.5 *

* At $W > 6\%$, to comply with the standard $CV_Q \leq 3\%$, it is necessary to increase ω to $3.0\text{--}3.5 \cdot \omega_{cr}$ or increase R_p to 0.20 m.

Analysis of Table 4 allows formulating three key quantitative conclusions:

1. At $\omega = 2.5 \cdot \omega_{cr}$ and $W \leq 6\%$, the standard $CV_Q \leq 3\%$ [1] is met for the entire moisture range.
2. Increasing moisture from 0 to 6% without loosener reduces flow rate from 8.35 to 3.87 kg/s (by a factor of 2.16); with loosener at $\omega = 2.5 \cdot \omega_{cr}$ – only from 8.35 to 8.15 kg/s (deviation 2.4%, within standard).
3. At $\omega < \omega_{cr}$, the loosener does not ensure mass flow even with increased drive power. Comparison of two pin arrangement schemes confirms the advantage of uniform 90° placement: the coefficient of variation of torque decreases from $CV \approx 60\%$ to $CV \approx 15\%$, which reduces the installed drive power by 28% (Fig. 6).

Conclusions.

1. It is theoretically substantiated that transitioning the flow regime of moist bulk materials of fraction 0–5 mm from funnel flow to mass flow without changing the standard geometry of BP hoppers ($\alpha = 60^\circ$) is possible by artificially reducing the effective internal friction angle ϕ_w below the critical ϕ_{cr} through continuous mechanical destruction of capillary bonds

From the normative requirement $CV_Q \leq 3\%$ [1] and substituting (18) into (19), we obtain the required loosener efficiency level $\eta(\omega) \geq 0.91$ at $\lambda = 0.091 \text{ \%}^{-1}$, $W_{max} = 8\%$. Substituting into (2.24) and solving for ω :

$$\omega op \geq \omega cr \cdot \left[1 - \left(\frac{1}{k\eta} \right) \cdot \ln(1 - 0.91) \right]^{-1} \approx 2.5 \cdot \omega cr \text{ at } k\eta = 2.8 \quad (20)$$

That is, to guarantee stable dosing at $W \leq 8\%$, the operating speed of the loosener with a horizontal shaft must exceed the threshold ω_{cr} by at least 2.5 times.

The consolidated mathematical model of material mass flow rate $Q_r(W, \omega, R_p)$ analytically links three groups of parameters: material properties (W, ρ, dp, λ), hopper geometry (B, k), and kinematic parameters of the loosener ($\omega, R_p, k\eta$):

by an active loosener with a horizontal shaft and 90° pin angular offset.

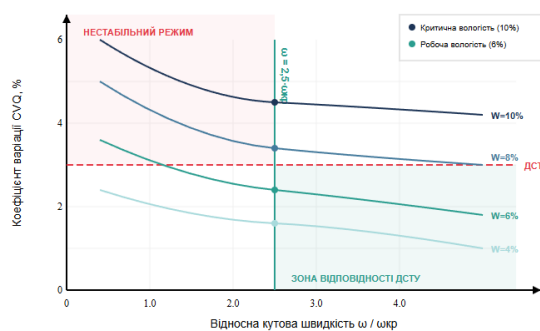


Figure 6. Dependence of mass flow rate coefficient of variation CV_Q on relative angular velocity ω/ω_{cr} at various sand moisture levels. Red dashed line – standard $CV_Q = 3\%$ (DSTU B V.2.7-96-2000 [1]). Vertical green line – $\omega = 2.5 \cdot \omega_{cr}$.

2. The physical mechanism of dynamic arch formation is established: at $W \geq 6\%$, cohesion $C(W) = 450\text{--}580$ Pa, critical outlet width $B_{cr} = 510\text{--}680$ mm exceeds the standard dimension (300 mm), which guarantees the formation of stable arches.

3. A design formula for the threshold angular velocity ω_{cr} (20) and a consolidated mathematical

model of mass flow rate $Q_r(W, \omega, R_p)$ (21) are obtained, forming the basis of an engineering design method for loosener parameters.

4. The practical condition for dosing stabilization is established: at $\omega_{op} \geq 2.5 \cdot \omega_{cr}$, $CV_Q \leq 3\%$ is ensured at

$W \leq 6\%$ in accordance with the requirements of DSTU B V.2.7-96-2000 [1]. The load uniformity coefficient $k_{uniform} = 0.72$ for 4 pairs of pins with 90° offset on a horizontal shaft provides 28% savings in peak drive load compared to non-uniform schemes.

References

1. DSTU B V.2.7-96-2000. (2000). *Будівельні матеріали. Заповнювачі пористі неорганічні для бетонів і будівельних розчинів. Метод контролю складу і фізико-механічних властивостей*. Держбуд України.
2. Sun, D., Huang, W., Liu, K., Ma, R., Wang, A., Guan, Y., & Shen, S. (2022). Effect of the moisture content of recycled aggregate on the mechanical performance and durability of concrete. *Materials*, 15(18), 6299. <https://doi.org/10.3390/ma15186299>
3. Khakhar, D., Yogi, J., & Momin, A. (2025). Computational and experimental analysis of granular flow in hoppers. *EPJ Web of Conferences*, 340, 01007. <https://doi.org/10.1051/epjconf/202534001007>
4. Schulze, D. (2021). *Powders and bulk solids: Behavior, characterization, storage and flow*. Springer. <https://doi.org/10.1007/978-3-540-73768-1>
5. Schulze, D. (2008). Flow properties of bulk solids. In D. Schulze, *Powders and bulk solids: Behavior, characterization, storage and flow* (pp. 35–74). Springer. https://doi.org/10.1007/978-3-540-73768-1_3
6. Barletta, D., & Poletto, M. (2012). Aggregation phenomena in fluidization of cohesive powders assisted by mechanical vibrations. *Powder Technology*, 225, 93–100. <https://doi.org/10.1016/j.powtec.2012.03.038>
7. Wes, G. (1990). Control of flow of cohesive powders by means of simultaneous aeration and vibration. *Powder Technology*, 61(1), 39–47. [https://doi.org/10.1016/0032-5910\(90\)80064-6](https://doi.org/10.1016/0032-5910(90)80064-6)
8. Huang, H., Zhang, Y., Wang, D., Fu, Z., Tian, H., Shang, J., Helal, M., & Lv, Z. (2024). Study the flow capacity of cylindrical pellets in hopper with unloading paddle using DEM. *Agriculture*, 14(4), Article 523. <https://doi.org/10.3390/agriculture14040523>
9. Jenike, A. W. (1964). *Storage and flow of solids* (Bulletin No. 123). University of Utah Engineering Experiment Station.
10. Lopes Neto, J. P., do Nascimento, J. W. B., Silva, R. C., & da Costa, C. A. (2013). Powder flow criteria for design of vertical silo walls. *Engenharia Agrícola*, 33(3), 453–462. <https://doi.org/10.1590/S0100-69162013000300003>
11. Brown, R. L., & Richards, J. C. (1970). *Principles of powder mechanics*. Pergamon Press.
12. Beverloo, W. A., Leniger, H. A., & van de Velde, J. (1961). The flow of granular solids through orifices. *Chemical Engineering Science*, 15(3–4), 260–269. [https://doi.org/10.1016/0009-2509\(61\)85030-6](https://doi.org/10.1016/0009-2509(61)85030-6)
13. Arnold, P. C., McLean, A. G., & Roberts, A. W. (1980). *Bulk solids: Storage, flow and handling*. TUNRA Bulk Solids Handling Research Associates.
14. Zhu, H. P., Zhou, Z. Y., Yang, R. Y., & Yu, A. B. (2007). Discrete particle simulation of particulate systems: Theoretical developments. *Chemical Engineering Science*, 62(13), 3378–3396. <https://doi.org/10.1016/j.ces.2006.12.089>
15. Levchenko, O., & Korobko, B. (2024). Optimization of the concrete production process in terms of energy consumption. *Technology Audit and Production Reserves*, 6(1), 11–15. <https://doi.org/10.15587/2706-5448.2024.319827>
1. DSTU B V.2.7-96-2000. (2000). *Building materials. Porous inorganic aggregates for concrete and mortars. Methods for controlling composition and physical and mechanical properties*. Derzhbud of Ukraine
2. Sun, D., Huang, W., Liu, K., Ma, R., Wang, A., Guan, Y., & Shen, S. (2022). Effect of the moisture content of recycled aggregate on the mechanical performance and durability of concrete. *Materials*, 15(18), 6299. <https://doi.org/10.3390/ma15186299>
3. Khakhar, D., Yogi, J., & Momin, A. (2025). Computational and experimental analysis of granular flow in hoppers. *EPJ Web of Conferences*, 340, 01007. <https://doi.org/10.1051/epjconf/202534001007>
4. Schulze, D. (2021). *Powders and bulk solids: Behavior, characterization, storage and flow*. Springer. <https://doi.org/10.1007/978-3-540-73768-1>
5. Schulze, D. (2008). Flow properties of bulk solids. In D. Schulze, *Powders and bulk solids: Behavior, characterization, storage and flow* (pp. 35–74). Springer. https://doi.org/10.1007/978-3-540-73768-1_3
6. Barletta, D., & Poletto, M. (2012). Aggregation phenomena in fluidization of cohesive powders assisted by mechanical vibrations. *Powder Technology*, 225, 93–100. <https://doi.org/10.1016/j.powtec.2012.03.038>
7. Wes, G. (1990). Control of flow of cohesive powders by means of simultaneous aeration and vibration. *Powder Technology*, 61(1), 39–47. [https://doi.org/10.1016/0032-5910\(90\)80064-6](https://doi.org/10.1016/0032-5910(90)80064-6)
8. Huang, H., Zhang, Y., Wang, D., Fu, Z., Tian, H., Shang, J., Helal, M., & Lv, Z. (2024). Study the flow capacity of cylindrical pellets in hopper with unloading paddle using DEM. *Agriculture*, 14(4), Article 523. <https://doi.org/10.3390/agriculture14040523>
9. Jenike, A. W. (1964). *Storage and flow of solids* (Bulletin No. 123). University of Utah Engineering Experiment Station.
10. Lopes Neto, J. P., do Nascimento, J. W. B., Silva, R. C., & da Costa, C. A. (2013). Powder flow criteria for design of vertical silo walls. *Engenharia Agrícola*, 33(3), 453–462. <https://doi.org/10.1590/S0100-69162013000300003>
11. Brown, R. L., & Richards, J. C. (1970). *Principles of powder mechanics*. Pergamon Press.
12. Beverloo, W. A., Leniger, H. A., & van de Velde, J. (1961). The flow of granular solids through orifices. *Chemical Engineering Science*, 15(3–4), 260–269. [https://doi.org/10.1016/0009-2509\(61\)85030-6](https://doi.org/10.1016/0009-2509(61)85030-6)
13. Arnold, P. C., McLean, A. G., & Roberts, A. W. (1980). *Bulk solids: Storage, flow and handling*. TUNRA Bulk Solids Handling Research Associates.
14. Zhu, H. P., Zhou, Z. Y., Yang, R. Y., & Yu, A. B. (2007). Discrete particle simulation of particulate systems: Theoretical developments. *Chemical Engineering Science*, 62(13), 3378–3396. <https://doi.org/10.1016/j.ces.2006.12.089>
15. Levchenko, O., & Korobko, B. (2024). Optimization of the concrete production process in terms of energy consumption. *Technology Audit and Production Reserves*, 6(1), 11–15. <https://doi.org/10.15587/2706-5448.2024.319827>

16. Petruniak, M., Rubel, V., Chevhanova, V., & Kulakova, S. (2021). Application of plugging solutions with the addition of defecate for effective well cementing. *Mining of Mineral Deposits*, 15(1), 59–65. <https://doi.org/10.33271/mining15.01.059>

16. Petruniak, M., Rubel, V., Chevhanova, V., & Kulakova, S. (2021). Application of plugging solutions with the addition of defecate for effective well cementing. *Mining of Mineral Deposits*, 15(1), 59–65. <https://doi.org/10.33271/mining15.01.059>

Левченко О.П.*

Національний університет «Полтавська політехніка імені Юрія Кондратюка»
<https://orcid.org/0009-0004-3191-7097>

Івахно О.В.

Національний університет «Полтавська політехніка імені Юрія Кондратюка»
<https://orcid.org/0009-0005-9375-8041>

Теоретичне обґрунтування параметрів системи живлення БЗУ для стабілізації масової витрати вологих матеріалів

Анотація. У статті теоретично обґрунтовано параметри системи живлення бетонозмішувальної установки для стабілізації масової витрати вологих дрібнозернистих заповнювачів фракції 0 - 5 мм. Встановлено, що при вологості піску $W \geq 4 - 6\%$ стандартна геометрія бункерів з кутом нахилу стінок $\alpha = 60^\circ$ не забезпечує масового режиму техніки за критерієм Дженіке, що зумовлює створення динамічних склепін і пульсуючу подачу матеріалу з коефіцієнтом варіації $CV = 15-25\%$. Сформульовано наукову гіпотезу про можливість переведення режиму течії з воронкового в масовий шляхом штучного зниження ефективного кута внутрішнього тертя нижче критичного значення за рахунок механічного руйнування капілярних зв'язків активним розпушувачем з горизонтальним валом та кутовим зміщенням штирів 90° . На основі теорії граничних рівноваг і рівняння Янссена з розрахунку когезії розроблено аналітичну модель формування динамічних склепін та отримано розрахункову формулу порогової кутової швидкості $\omega_{кр}$. Побудовано зведену математичну модель масових витрат матеріалу. Встановлено, що при робочій швидкості $\omega_{пр} \geq 2,5 \cdot \omega_{кр}$ досягається коефіцієнт варіації масової витрати $CVQ \leq 3\%$ при $W \leq 6\%$ відповідно до вимог ДСТУ Б В.2.7-96-2000.

Ключові слова: насос, бетонозмішувальна установка, розпушувач, склепіння, когезія, вологість, дозування, бункер, витрата, кутова швидкість, течія

*Адреса для листування E-mail: volodimirantonchik1958@gmail.com

Надіслано до редакції:	08.02.2026	Прийнято до друку після рецензування:	12.04.2026	Опубліковано (оприлюднено):	31.05.2026
------------------------	------------	---------------------------------------	------------	-----------------------------	------------

Suggested Citation:

APA style Levchenko, O., & Ivakhno, O. (2026). Theoretical substantiation of the parameters of the concrete batching plant feeding system for stabilising the mass flow rate of moist materials. *Academic Journal. Industrial Machine, Building Civil Engineering*, 1(66), 139–145. <https://doi.org/10.26906/znp.2026.66.4352>

DSTU style Levchenko O., Ivakhno O. Theoretical substantiation of the parameters of the concrete batching plant feeding system for stabilising the mass flow rate of moist materials. *Academic journal. Industrial Machine Building, Civil Engineering*. 2026. Vol. 66, iss. 1. P. 139–145. URL: <https://doi.org/10.26906/znp.2026.66.4352>.